Available online at www.sciencedirect.com
ScienceDirect
Journal of Sound and Vibration 318 (2008) 850–867
JOURNAL OF SOUND AND VIBRATION
www.elsevier.com/locate/jsvi

Free in-plane vibration of general curved beams using finite element method

F. Yang[a], R. Sedaghati[a], E. Esmailzadeh[b,*]

[a]*Department of Mechanical and Industrial Engineering, Concordia University, 1455 de Maisonneuve Blvd. West, Montreal, Quebec, Canada H3G 1M8*

[b]*Faculty of Engineering and Applied Science, University of Ontario Institute of Technology, 2000 Simcoe Street North, Oshawa, Ontario, Canada L1H 7K4*

Received 21 May 2007; received in revised form 18 April 2008; accepted 22 April 2008
Handling Editor: S. Bolton
Available online 6 June 2008

Abstract

The governing differential equations for the free in-plane vibration of uniform and non-uniform curved beams with variable curvatures, including the effects of the axis extensibility, shear deformation and the rotary inertia, are derived using the extended-Hamilton principle. These equations were then solved numerically utilizing the Galerkin finite element method and the curvilinear integral taken along the central line of the curvilinear beam. Based on the proposed finite element formulation, one can easily study curved beams having different geometrical and boundary conditions. Furthermore, those curved beams, excluding the effects of the axis extensibility, shear deformation and the rotary inertia, are modeled and then solved utilizing the finite element method using a new non-isoparametric element. The results for the natural frequencies, modal shapes and the deformed configurations are presented for different types of the curved beams with various geometrical properties and boundary conditions, and in order to illustrate the validity and accuracy of the presented methodology they are compared with those published in literature.

1. Introduction

The study of the free in-plane vibration of a curved beam using the beam theory is more complex than the analogous problem in a straight beam, since the structural deformations in a curved beam depends not only on the rotation and radial displacements but also on the coupled tangential displacement caused by the curvature of the structure. Many theories have been evolved to derive, simplify and solve the equations of motion for the free in-plane vibration of the curved beams. Most of the studies are generally focused on the uniform circular arc, and the relative equations of motion are solved using the Rayleigh–Ritz method. Henrych [1] derived the general expression of the equations of motion for a uniform circular arc based on the first-order equilibrium condition. Auciello and Rosa [2] ignored the shear deformation and rotary inertia, and assumed that the curved axis is incompressible. Veletsos and Austin [3] disregarded the shear deformation and the extensibility

*Corresponding author. Tel.: +1 905 721 3111; fax: +1 905 721 3370.
E-mail address: ezadeh@uoit.ca (E. Esmailzadeh).

0022-460X/$ - see front matter © 2008 Elsevier Ltd. All rights reserved.
doi:10.1016/j.jsv.2008.04.041

Nomenclature

A	cross-sectional area of beam
E	elastic modulus
G	shear modulus
I	area moment of inertia of beam
J	mass moment of inertia density of Timoshenko beam
k_q	sectional shear coefficient of the curved beam
l	length of the curved beam
L	span length of the curved beam
m	density per unit length of beam
$\mathbf{M}$ and $\mathbf{K}$	mass and stiffness matrices
S	curvilinear coordinate
T	kinetic energy
$\mathbf{u}$	tangential displacement
V	potential energy
$\mathbf{w}$	radial displacement
β	beam rotation due to shear
γ	density of material
η	natural coordinates
φ	rotation due to tangential displacement
$\mathbf{\Psi}$	beam rotation due to bending

of the curve axis and assumed that the tangential and the radial displacements are uncoupled. Wolf [4] analyzed the free vibration of elastic circular arches using 99 straight Euler–Bernoulli beam segments to approximate the arch. Eisenberger and Efraim [5] studied the uniform circular beams using the Timoshenko beam theory, which includes the effects of rotary inertia, shear deformation, and the couplings of the radial and tangential displacements.

It has been shown that the Timoshenko beam theory provides a better approximation to the actual behavior of beams, in which the effect of the cross-sectional dimension on frequencies cannot be neglected, and the study of high modes is required. Friedman and Kosmatka [6] utilized the Ritz method based on the trigonometric functions and derived the exact static stiffness matrix for the uniform circular curved beams. Kang et al. [7] utilized the differential quadrate method (DQM) to compute the eigenvalues of the equations of motion governing the uniform circular curved beams.

Irie et al. [8] and also Yildirim [9] solved the equations of motion using the transfer matrix method and Veletsos and Austin [3] presented the numerical solutions for the first eight lowest natural frequencies of circular arches. Subsequently, they investigated the effects of the previously neglected factors (the rotary inertia and the shear deformation) and developed an approximate and simplified procedure to estimate the natural frequencies of the circular arches [10]. The general dynamic stiffness matrix for a uniform circular curved beam was derived by Issa et al. [11].

For a non-uniform circular beam, Laura and Verniere [12] studied a circular beam with linear varying thickness. Tong et al. [13] ignored the shear deformation and rotary inertia, and assumed the incompressible curve axis. ÖztÜrk et al. [14] ignored the shear deformation and the extensibility of the curve axis but they assumed that the tangential and radial displacements are uncoupled. Lee and Hsiao [15] ignored the shear deformation and the extensibility of curved axis. For the non-circular arches, Tseng et al. [16] analyzed the parabolic and elliptic arches to obtain their natural frequencies. The natural frequencies for the elliptical, parabolic and sinusoidal arches were also found by Oh et al. [17].

Utilizing finite element (FE) method to solve the curved beams problem can be found in some published papers. Friedman and Kosmatka [6] utilized the trigonometric functions as the interpolation function and their approach was basically based on the Ritz method. Raveendranath et al. [18] utilized three kinds of two-node elements to study the curved beam. Litewka and Rakowski [19] utilized the same interpolation function given in Ref. [6]. Wu and Chiang [20] presented a set of interpolation function based on Ref. [6], while ÖztÜrk et al. [14] utilized a set of trigonometric functions as the interpolation function. In fact, the interpolation (shape) function utilized in many publications in relation with the FE method in curved beams are based on two published papers by Petyr and Fleischer [21] and Davis et al. [22]. All these papers utilized the two-node element to study the circular curved beam. For the circular curved beam, the radius of curvature is constant (R) and thus the problem can be simplified by interchanging the curvilinear coordinates s with the arch angle (θ).

It can be realized that not much work has been done on either uniform or non-uniform curved beams with variable curvatures. In particular, no further work based on the FE approach has been reported on these types of structure. Considering this fact, the main objective of this study is to develop the FE model for the general curved beams with variable curvature and for both uniform or non-uniform cross-sectional areas and different boundary conditions. The governing equations of motion are derived using the extended-Hamilton principle and then the weighted residual technique, based on the Galerkin method, is utilized to transfer the governing equations into the FE form. Initially, the FE model of the curved beam including the effect of the axis extensibility, shear deformation and the rotary inertia (Case 1) is developed. Subsequently, the curved beam has been modeled as an inextensible beam, in which the effects of the shear deformation and the rotary inertia are neglected (Case 2).

An innovative FE method is presented to solve the curved beam problems for Case 2. Efficient numerical techniques, based on the curvilinear integral taken along the central line of the curvilinear beam, and the Gaussian integral method [23] have been implemented to solve the governing FE equations. The results for the natural frequencies, modal shapes and the deformed configurations of different curved beams with different boundary condition are obtained and compared with those reported in literature.

2. Mathematical modeling

The geometry of the general symmetric curved beam is illustrated in Fig. 1. Two different cases will be investigated in this study: Case 1—the effects of the extensibility of the curved axis, shear deformation, and the rotary inertia are all considered; and Case 2—all these effects have been totally ignored. The geometrical and deformational relationships for both Cases are summarized in Table 1.

The parameters L, Φ and h in Fig. 1 and Table 1 are the span length, the curve angle, and the rise of the curved beam, respectively. The coordinate S is along the central line and $y(x)$ is the function describing the central line. Parameters $w(s)$, $u(s)$, $\varphi(s)$, $\psi(s)$ and $\beta(s)$ are the respective beam radial displacement, the tangential displacement, the rotation due to the tangential displacement, the rotation due to the bending and the rotation due to the shear along the S coordinate. Furthermore, $\rho(s)$, u_T(s), $\mathrm{d}w(s)/\mathrm{d}s$ and $w(s)/\rho(s)$ are the curved beam radius of curvature, the beam total tangential displacement, the total rotation and the tangential displacement due to the radial displacement along the S coordinate, respectively.

The extended-Hamilton theory principle was used to derive the governing differential equations of motion:

$$\int_{t_1}^{t_2} (\delta T - \delta V + \delta W_{nc})\,\mathrm{d}t = 0, \quad \delta(.) = 0 \ \text{ at } \ t = t_1, t_2, \tag{1}$$

where the kinetic energy (T) and the potential energy (V) in its most general form (Case 1) can be written as

$$T = \frac{1}{2}\int_L m(s)\left(\frac{\partial w(s,t)}{\partial t}\right)^2 \mathrm{d}s + \frac{1}{2}\int_L J(s)\left(\frac{\partial \psi(s,t)}{\partial t}\right)^2 \mathrm{d}s + \frac{1}{2}\int_L m(s)\left(\frac{\partial u(s,t)}{\partial t}\right)^2 \mathrm{d}s \tag{2}$$

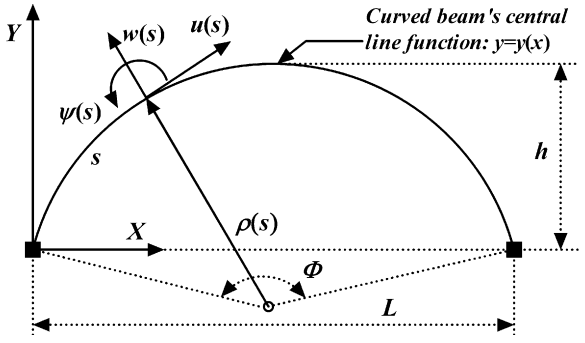

Fig. 1. Curved beam geometry.

Table 1
Geometrical and deformational relationships for Cases 1 and 2

	Case 1	Case 2
Radial displacement	$w(s)$	$w(s)$
Differential of the tangential displacement	$\mathrm{d}u_T(s)/\mathrm{d}s = \mathrm{d}u(s)/\mathrm{d}s+w(s)/\rho(s)$	$0 = \mathrm{d}u(s)/\mathrm{d}s+w(s)/\rho(s)$
Rotation due to the tangential displacement	$\varphi(s) = u(s)/\rho(s)$	$\varphi(s) = u(s)/\rho(s)$
Total rotation	$\mathrm{d}w(s)/\mathrm{d}s = \beta(s)+\psi(s)+\varphi(s)$	$\mathrm{d}w(s)/\mathrm{d}s = \psi(s)+\varphi(s)$

and

$$V = \frac{1}{2}\int_L EI(s)\left(\frac{\partial\psi(s,t)}{\partial s}\right)^2 \mathrm{d}s + \frac{1}{2}\int_L k_q GA(s)\beta^2(s,t)\,\mathrm{d}s + \frac{1}{2}\int_L EA(s)\left(\frac{\partial u_T(s,t)}{\partial s}\right)^2 \mathrm{d}s, \tag{3}$$

where parameters $m(s)$ and $J(s)$ are the respective density per unit length and the mass moment of inertia density along the S coordinate and E, G and k_q are the elastic modulus, the shear modulus and the sectional shear coefficient of beams, respectively.

The integral ($\int_L[.]$) represents the curvilinear integral taken along the S coordinate. It should be noted that the mass moment of inertia density, $J(s)$, is related to the area moment of inertia, $I(s)$, and the beam material density, $\gamma(s)$, along the central line of the curvilinear beam by the equation $J(s) = \gamma(s)I(s)$. Here, the non-conservative virtual work is assumed to be zero as the main purpose of this study is to obtain the natural frequencies of the curved beams.

The geometrical and deformational expressions for Case 1, listed in Table 1, were substituted into Eqs. (2) and (3), and by identifying $w(s)$, $u(s)$ and $\psi(s)$ as the independent variables, and applying Hamilton's principle stated in Eq. (1), the following three governing differential equations of motion will be obtained for Case 1 as

$$-m(s)\frac{\partial^2 w(s,t)}{\partial t^2} + \frac{\partial}{\partial s}\left\{k_q GA(s)\left[\frac{\partial w(s,t)}{\partial s} - \frac{u(s,t)}{\rho(s)} - \psi(s,t)\right]\right\} - \frac{EA(s)}{\rho(s)}\left[\frac{\partial u(s,t)}{\partial s} + \frac{w(s,t)}{\rho(s)}\right] = 0, \tag{4a}$$

$$-m(s)\frac{\partial^2 u(s,t)}{\partial t^2} + \frac{k_q GA(s)}{\rho(s)}\left[-\psi(s,t) + \frac{\partial w(s,t)}{\partial s} - \frac{u(s,t)}{\rho(s)}\right] + \frac{\partial}{\partial s}\left\{EA(s)\left[\frac{\partial u(s,t)}{\partial s} + \frac{w(s,t)}{\rho(s)}\right]\right\} = 0, \tag{4b}$$

$$-J(s)\frac{\partial^2 \psi(s,t)}{\partial t^2} + \frac{\partial}{\partial s}\left(EI(s)\frac{\partial\psi(s,t)}{\partial s}\right) + k_q GA(s)\left[\frac{\partial w(s,t)}{\partial s} - \psi(s,t) - \frac{u(s,t)}{\rho(s)}\right] = 0. \tag{4c}$$

The FE model of the system will now be developed based on Eqs. (4). By using the natural coordinate system and the appropriate Lagrangian-type shape functions, the Cartesian coordinate ($x(s)$ and $y(s)$), the radial displacement, $w(s)$, the tangential displacement, $u(s)$, the rotation due to bending, $\psi(s)$, the cross-sectional area, $A(s)$, and the area moment of inertia, $I(s)$, can be related to their relative nodal values as

$$\begin{aligned} &x(\eta) = \mathbf{N}(\eta)\mathbf{x}, \quad y(\eta) = \mathbf{N}(\eta)\mathbf{y}, \quad w(\eta,t) = \mathbf{N}(\eta)\mathbf{w}(t), \\ &u(\eta,t) = \mathbf{N}(\eta)\mathbf{u}(t), \quad \psi(\eta,t) = \mathbf{N}(\eta)\boldsymbol{\psi}(t), \quad A(\eta) = \mathbf{N}(\eta)\mathbf{A}, \quad I(\eta) = \mathbf{N}(\eta)\mathbf{I}, \end{aligned} \tag{5}$$

where η is the natural coordinate ($-1 \leqslant \eta \leqslant 1$) and $\mathbf{N}(\eta)$ is the Lagrangian-type shape function matrix and the state vectors $\mathbf{w}(t)$, $\mathbf{u}(t)$ and $\boldsymbol{\psi}(t)$ are the respective nodal radial displacement, the nodal tangential displacement, and the nodal rotation vectors associated with the radial displacement function, w, the tangential displacement function, u, and the rotation function, ψ. Similarly, $\mathbf{x}$, $\mathbf{y}$, $\mathbf{A}$ and $\mathbf{I}$ are the nodal values associated with the x, y, A and I functions, respectively.

By applying the Galerkin weighted residual technique to Eqs. (4), substituting the relative functions with respect to their nodal values as given in Eq. (5), and then utilizing the Jacobin relationship between the Cartesian coordinate (X and Y), the curvilinear coordinate, S, and the natural coordinate, η, the following governing equation of motions in the FE form can be obtained:

$$\mathbf{M} \times \ddot{\mathbf{q}}(t) + \mathbf{K} \times \mathbf{q}(t) = 0, \tag{6}$$

where

$$\mathbf{q} = \{\, \mathbf{w}(t) \quad \mathbf{u}(t) \quad \boldsymbol{\psi}(t) \,\}^{\mathrm{T}}, \tag{6a}$$

$$\mathbf{M} = \begin{bmatrix} \mathbf{M}_{\mathbf{ww}} & \mathbf{0} & \mathbf{0} \\ \mathbf{0} & \mathbf{M}_{\mathbf{uu}} & \mathbf{0} \\ \mathbf{0} & \mathbf{0} & \mathbf{M}_{\boldsymbol{\psi}\boldsymbol{\psi}} \end{bmatrix}, \tag{6b}$$

$$\mathbf{K} = \begin{bmatrix} \mathbf{K}_{\mathbf{ww}} & \mathbf{K}_{\mathbf{wu}} & \mathbf{K}_{\mathbf{w}\boldsymbol{\psi}} \\ \mathbf{K}_{\mathbf{wu}}^{\mathrm{T}} & \mathbf{K}_{\mathbf{uu}} & \mathbf{K}_{\mathbf{u}\boldsymbol{\psi}} \\ \mathbf{K}_{\mathbf{w}\boldsymbol{\psi}}^{\mathrm{T}} & \mathbf{K}_{\mathbf{u}\boldsymbol{\psi}}^{\mathrm{T}} & \mathbf{K}_{\boldsymbol{\psi}\boldsymbol{\psi}} \end{bmatrix}. \tag{6c}$$

The mass and stiffness sub-matrices given by Eqs. (6b) and (6c) are compiled in Appendix A, and using the Gauss quadrate technique and the curvilinear integral taken along the central line of curvilinear beam they were evaluated numerically.

Ignoring the axis extensibility, the shear deformation, and the rotary inertia (Case 2), the kinetic energy (T) and the potential energy (V) can be simplified as

$$T = \frac{1}{2}\int_L m(s)\left(\frac{\partial w(s,t)}{\partial t}\right)^2 \mathrm{d}s + \frac{1}{2}\int_L m(s)\left(\frac{\partial u(s,t)}{\partial t}\right)^2 \mathrm{d}s \tag{7}$$

and

$$V = \frac{1}{2}\int_L EI(s)\left(\frac{\partial \psi(s,t)}{\partial s}\right)^2 \mathrm{d}s. \tag{8}$$

Substituting the geometrical and deformation relationships for Case 2, as listed in Table 1, into Eqs. (7) and (8) and selecting $w(s)$ and u(s) as the variables and then applying the Hamilton's principle stated in Eq. (1), the following two governing differential equations for Case 2 can be obtained:

$$m(s)\frac{\partial^2 w(s,t)}{\partial t^2} + \frac{\partial^2}{\partial s^2}\left(EI(s)\frac{\partial^2 w(s,t)}{\partial s^2}\right) - \frac{\partial^2}{\partial s^2}\left(\frac{EI(s)}{\rho(s)}\frac{\partial u(s,t)}{\partial s}\right) = 0, \tag{9a}$$

$$m(s)\frac{\partial^2 u(s,t)}{\partial t^2} + \frac{\partial}{\partial s}\left(\frac{EI(s)}{\rho(s)}\frac{\partial^2 w(s,t)}{\partial s^2}\right) - \frac{\partial}{\partial s}\left(\frac{EI(s)}{\rho^2(s)}\frac{\partial u(s,t)}{\partial s}\right) = 0. \tag{9b}$$

These two equations can be combined utilizing the incompressible assumption for Case 2 to obtain a single governing differential equation of order 6 with respect to the tangential displacement, u [1]. The FE model of the system can simply be developed based on Eqs. (9). For this case, the Lagrangian-type shape function, similar to Case 1, is utilized to relate the Cartesian coordinate ($x(s)$ and $y(s)$), the cross-sectional area function, $A(s)$ and the area moment of inertia function, $I(s)$, to their relative nodal values of $\mathbf{x}$, $\mathbf{y}$, $\mathbf{A}$ and $\mathbf{I}$:

$$x(\eta) = \mathbf{N}(\eta)\mathbf{x}, \quad y(\eta) = \mathbf{N}(\eta)\mathbf{y}, \quad \mathbf{A}(\eta) = \mathbf{N}(\eta)\mathbf{A}, \quad \mathbf{I}(\eta) = \mathbf{N}(\eta)\mathbf{I}, \tag{10}$$

A polynomial equation of order 5 would then be used to describe the tangential displacement for this case as it will satisfy the governing differential equation with respect to the tangential displacement obtained by combining Eqs. (9) as

$$u(\eta) = c_0 + c_1\eta + c_2\eta^2 + c_3\eta^3 + c_4\eta^4 + c_5\eta^5. \tag{11}$$

Using Table 1 for Case 2, the radial displacements and the rotations are related to the tangential displacements as

$$w(\eta) = -\frac{\mathrm{d}u}{\mathrm{d}\eta}\frac{\rho(\eta)}{J_{oc}(\eta)} \text{ and } \psi(\eta) = \frac{\mathrm{d}w}{\mathrm{d}\eta}\frac{1}{J_{oc}(\eta)} - \frac{u(\eta)}{\rho(\eta)}, \tag{12}$$

where the Jacobian, $J_{oc}(\eta)$, can be obtained using

$$J_{oc}(\eta) = \frac{\mathrm{d}s}{\mathrm{d}\eta} = \sqrt{\left(\frac{\mathrm{d}x}{\mathrm{d}\eta}\right)^2 + \left(\frac{\mathrm{d}y}{\mathrm{d}\eta}\right)^2} = \sqrt{(\mathbf{B}(\eta)\mathbf{x})^2 + (\mathbf{B}(\eta)\mathbf{y})^2}, \tag{13}$$

where $\mathbf{B}(\eta) = \mathrm{d}(\mathbf{N}(\eta))/\mathrm{d}\eta$.

The displacement function, $u(\eta)$, can be related to the six degrees-of-freedom (dof) of the two-node curved beam element (each node has three dof u, w, ψ) with nodes i and j by using Eqs. (11)–(13), as

$$u(\eta) = \mathbf{N}_N\{\, u_i \quad w_i \quad \psi_i \quad u_j \quad w_j \quad \psi_j \,\}^{\mathrm{T}}, \tag{14}$$

where $\mathbf{N}_N$ is the shape function matrix, which can be calculated from Eqs. (10) to (14). It is noted that the radius of curvature can be evaluated from the expression

$$\frac{1}{\rho} = \frac{y''}{(1+y'^2)^{1.5}}. \tag{15}$$

Finally, by applying the Galerkin weighted residual technique to the governing differential equations stated in Eq. (9), the FE form of the governing equations for Case 2, similar to Eq. (6), derived for Case 1, can be obtained. The nodal displacement vector and the mass and the stiffness matrices for this case can be expressed as

$$\mathbf{q} = \{u_1, w_1, \psi_1, \ldots, u_n, w_n, \psi_n\}^{\mathrm{T}}, \tag{16}$$

$$\mathbf{M} = \sum_{\text{element}} \left\{ \int_{-1}^{1} \left\{ \begin{array}{c} \dfrac{\rho^2(\eta)}{J_{oc}(\eta)} \mathbf{B}_N(\eta)^{\mathrm{T}} \gamma \mathbf{N}(\eta) \mathbf{A} \mathbf{B}_N(\eta) \\ +\rho^2(\eta) \mathbf{N}_N(\eta)^{\mathrm{T}} \gamma \mathbf{N}(\eta) \mathbf{A} \mathbf{N}_N(\eta) J_{oc}(\eta)) \end{array} \right\} \mathrm{d}\eta \right\}, \tag{17}$$

$$\mathbf{K} = \sum_{\text{element}} \left\{ \int_{-1}^{1} \left\{ \begin{array}{l} \dfrac{\rho(\eta)}{J_{oc}^5(\eta)} \mathbf{D}_N(\eta)^{\mathrm{T}} E\mathbf{N}(\eta) \mathbf{I} \mathbf{D}_N(\eta) + \dfrac{E\mathbf{N}(\eta)\mathbf{I}}{J_{oc}^3(\eta)} \mathbf{D}_N(\eta)^{\mathrm{T}} \mathbf{B}_N(\eta) \\ +\dfrac{E\mathbf{N}(\eta)\mathbf{I}}{J_{oc}^3(\eta)} \mathbf{B}_N(\eta)^{\mathrm{T}} \mathbf{D}_N(\eta) + \dfrac{E\mathbf{N}(\eta)\mathbf{I}}{\rho^2(\eta) J_{oc}(\eta)} \mathbf{B}_N(\eta)^{\mathrm{T}} \mathbf{B}_N(\eta) \end{array} \right\} \mathrm{d}\eta \right\} \tag{18}$$

where n is the total number of nodes to model the curved beam and $\mathbf{B}_N(\eta) = \mathrm{d}(\mathbf{N}_N(\eta))/\mathrm{d}\eta$, $\mathbf{D}_N(\eta) = \mathrm{d}^3(\mathbf{N}_N(\eta))/\mathrm{d}\eta^3$.

3. Numerical results

In this section, illustrative examples are presented to illustrate the generality and accuracy of the developed methodology. In order to investigate the effects of the shear deformation, rotary inertia and the axis extensibility, detailed comparisons of the results are presented for both Cases 1 and 2. All the curved beams studied for Case 1, are modeled using 10 'curved beam elements' each having 4 nodes per element. Furthermore, 10 'curved beam elements' (4 nodes per element) are used for Case 2 to evaluate the nodal cross-sectional area and the moment of inertia, the radius of curvature, and the geometrical Jacobian matrix, and then '10 curved beam elements' (2 nodes per element), as illustrated in Eq. (14), are employed to evaluate the nodal displacement vectors for Case 2.

3.1. Extensible curved beam model with the shear deformation and rotary inertia (Case 1)

Here, using the developed methodology, several examples are studied. The examples range from a simple circular arch to parabolic, elliptical, and the sinusoidal and general curved arches.

Example 1. Uniform circular curved beam with pinned–pinned boundary conditions.

The uniform circular curved beam with the pinned–pinned boundary condition is considered here. The beam has the following material and geometrical characteristics:

$$R/r = 15, \quad l/r = 23.56, \quad \Phi = 90^\circ, \quad R = 0.75\,\mathrm{m}, \quad A = 4\,\mathrm{m}^2, \quad I = 0.01\,\mathrm{m}^4,$$
$$E = 70\,\mathrm{GPa}, \quad k_q = 0.85, \quad k_q G/E = 0.3, \quad \gamma = 2777\,\mathrm{kg/m}^3,$$

where R, $r = \sqrt{(I/A)}$, $l = R\Phi$ and γ are the radius of the circle, the radius of gyration, the length of the curved beam and the material density, respectively.

The result for the first 10 non-dimensional natural frequencies, λ, ($\lambda = \omega l^2\sqrt{(\gamma A/EI)}$) are listed in Table 2, and the associated modal shapes and the deformed configurations are illustrated in Figs. 2 and 3, respectively. It can be realized that very close agreement between the present results and those published in Refs. [5,10] does exist. It should be noted that in the modal shape figures, the horizontal axis ''non-dimension beam curvilinear length'' is defined by the non-dimensional parameter s/l in which, s is the location along the curved beam central line. Therefore, s/l varies between zero and one.

Example 2. Uniform circular curved beam with clamped–clamped boundary conditions.

In this example, a uniform circular curved beam with the clamped–clamped boundary is studied. The geometrical and material properties are

$$R/r = 15.915, \quad l/r = 25, \quad \Phi = 90^\circ, \quad R = 0.6366\,\mathrm{m}, \quad A = 1\,\mathrm{m}^2, \quad I = 0.0016\,\mathrm{m}^4,$$
$$E = 70\,\mathrm{GPa}, \quad k_q = 0.85, \quad k_q G/E = 0.3, \quad \gamma = 2777\,\mathrm{kg/m}^3.$$

The results for the first 10 non-dimensional natural frequencies (λ) are listed in Table 3, and the associated modal shapes and the deformed configurations are presented in Figs. 4 and 5, respectively. Once again, as it can be seen the results are in very close agreement with those reported in Refs. [5,10].

Example 3. Parabolic, elliptical and sinusoidal uniform curved beams.

In this example, the parabolic, elliptical and the sinusoidal arches, shown in Fig. 6, are investigated for their natural frequencies. To facilitate the numerical study, the following non-dimensional variables are defined: $f = h/L$ (arch rise to the span length), $\mathrm{SR} = L/\sqrt{(I/A)}$ (slenderness ratio) and $\xi = x/L$. The cross-sectional area, the second moment of area of the beam, and all the beam material properties are similar to those given in Example 1.

The non-dimensional equation for the parabolic arch (Fig. 6a) is defined as [17]

$$y = 4f\xi(1-\xi), \quad 0 < \xi < 1. \tag{19}$$

The non-dimensional equation for the sinusoidal arch (Fig. 6b) is defined as [17]

$$y = f - c_1 + c_1 \sin(c_2\xi + \varepsilon c_2), \quad 0 < \xi < l, \tag{20}$$

Table 2
Non-dimensional frequencies $\lambda = \omega l^2\sqrt{(\gamma A/EI)}$ of a uniform circular curved beam with the pinned–pinned boundary conditions (Case 1)

Mode	Ref. [5]	Ref. [10]	Present study
1	29.280	29.61	29.306
2	33.305	33.01	33.243
3	67.124	67.24	67.123
4	79.971	79.6	79.950
5	107.851	107.7	107.844
6	143.618	144.5	143.679
7	156.666	155.2	156.629
8	190.477	191.3	190.596
9	225.361	223.7	225.349
10	234.524	235.3	234.809

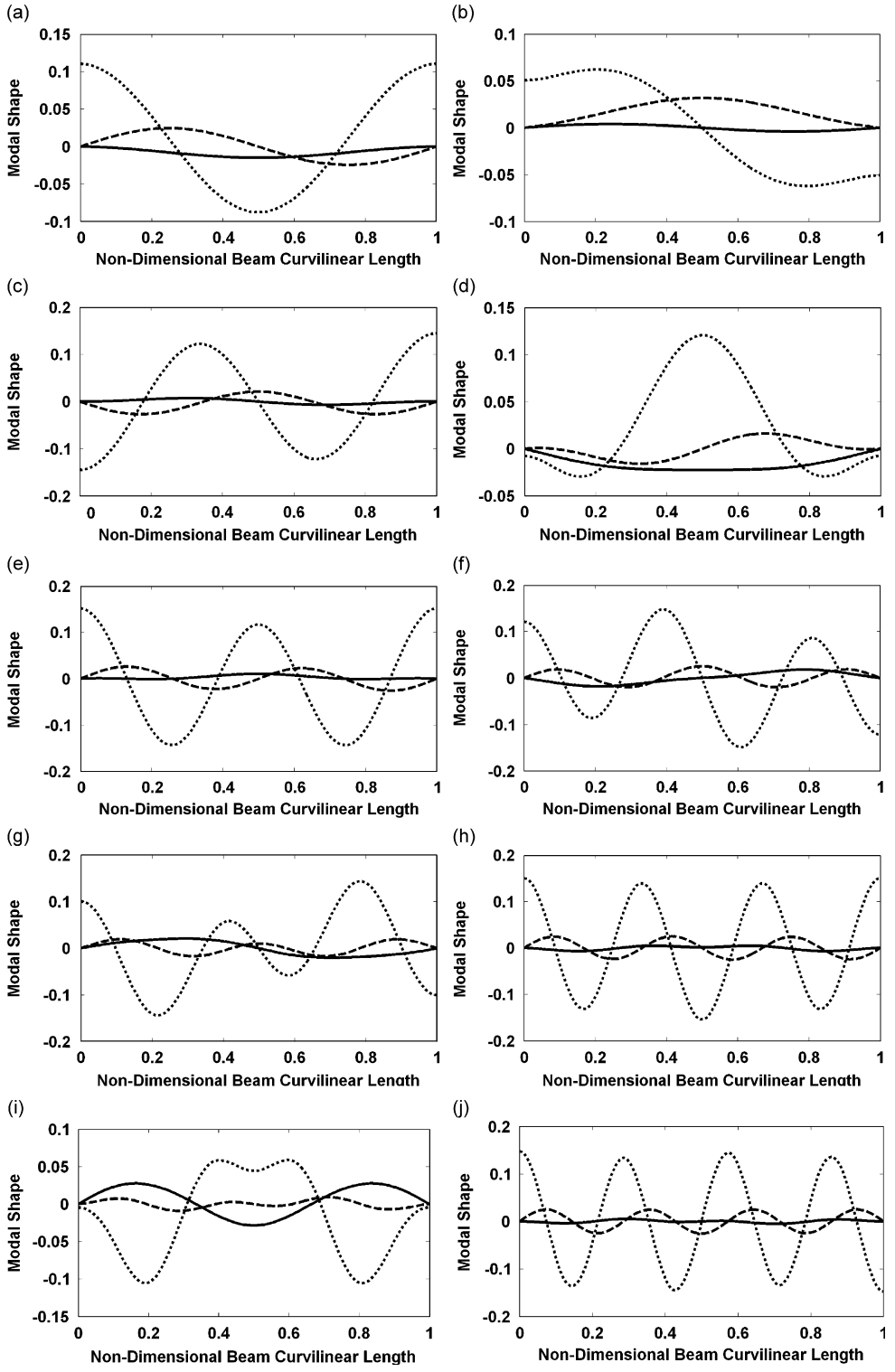

Fig. 2. The first 10 vibration modal shapes of uniform circular curved beam with pined–pined boundary conditions. Solid, dashed and dotted lines represent mode shapes for u, w and ψ, respectively: (a) the first mode, (b) the second mode, (c) the third mode, (d) the forth mode, (e) the fifth mode, (f) the sixth mode, (g) the seventh mode, (h) the eighth mode, (i) the ninth mode and (j) the tenth mode.

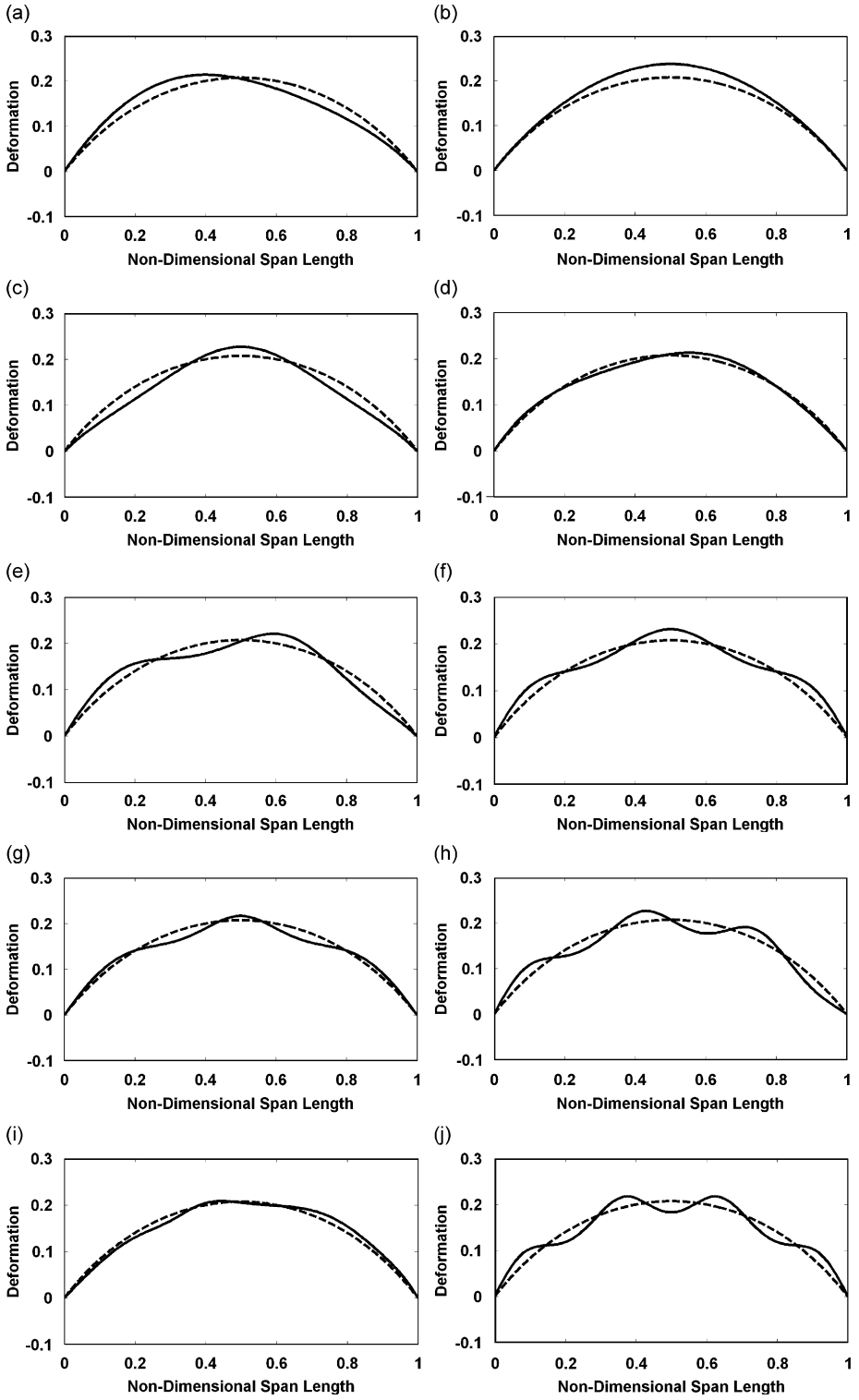

Fig. 3. The deformations relative to the first 10 vibration modes for uniform circular curved beam with pined–pined boundary conditions. Solid and dashed lines represent deformed and undeformed configuration: (a) the first mode, (b) the second mode, (c) the third mode, (d) the forth mode, (e) the fifth mode, (f) the sixth mode, (g) the seventh mode, (h) the eighth mode, (i) the ninth mode, and (j) the tenth mode.

Table 3
Non-dimensional frequencies $\lambda = \omega l^2\sqrt{(\gamma A/EI)}$ of uniform circular curved beam with clamped–clamped boundary conditions (Case 1)

Mode	Ref. [5]	Ref. [10]	Present study
1	36.703	36.81	36.657
2	42.264	42.44	42.289
3	82.233	82.5	82.228
4	84.491	84.3	84.471
5	122.305	122.5	122.298
6	154.945	155.1	154.998
7	168.203	167.7	168.174
8	204.472		204.599
9	238.992		238.973
10	249.011	249.6	249.320

where

$$c_2 = \pi/(1+2\varepsilon), \quad c_1 = f/[1-\sin(\varepsilon c_2)]. \tag{21}$$

The non-dimensional equation for the elliptical arch (Fig. 6c) can be written as

$$y = b_2\sqrt{1-\{1-[\xi - b_1\cos(a)]/b_1\}^2} - b_2\sin(a), \quad 0<\xi<1, \tag{22}$$

where

$$b_1 = \varepsilon + 0.5, \quad a = \arccos(0.5/b_1), \quad b_2 = f/[1-\sin(a)]. \tag{23}$$

The numerical results for the first four non-dimensional natural frequencies, $\lambda = \omega L^2\sqrt{(\gamma A/EI)}$ are listed in Table 4. Results are also in excellent agreement with those reported in Ref. [17].

Example 4. General non-uniform and non-circular curved beams.

To demonstrate the generality of the developed methodology, a general curved beam with the clamped–clamped boundary condition, shown in Fig. 7, representing an overpass bridge is investigated. It should be noted this type of curved beam has a variable radius of curvature and also the cross-sectional area and the area moment of inertia of the beam would vary along the curvilinear central line. The physical properties of the curved beam are listed in Table 5.

The variations of the first four natural frequencies with respect to the number of elements are shown in Fig. 8. It can be realized that the natural frequencies converge rapidly with the increase in the number of elements. As can be seen, there is no significant changes in the natural frequencies when choosing the number of elements higher than 6. The first four associated modal shapes of vibration and the beam deformations are illustrated in Figs. 9 and 10, respectively.

3.2. Inextensible uniform curved beam with no shear deformation and rotary inertia (Case 2)

The natural frequencies of a uniform circular beam is once again studied here but this time the effect of the extensibility, the shear deformation and the rotary inertia of the beam have all been ignored. The parameters related to the tangential inertial force, which are presented in Eqs. (7), (9) and (17), have also been ignored in order to compare the result with those reported in literature [1]. The circular beams with different boundary conditions and different curved angle (Φ) are analyzed. The 10 non-dimensional natural frequencies ($\lambda = \omega R^2\sqrt{(\gamma A/EI)}$) of the circular beam with various curve angles and different boundary conditions are listed in Tables 6–9, and they were compared with their corresponding values published in Ref. [1].

The last columns of Tables 6 and 7 are the non-dimensional natural frequencies defined by $\lambda = \omega l^2\sqrt{(\gamma A/EI)}$ for the pinned–pinned and the clamped–clamped circular beam with the curve angle $\Phi = 90^\circ$, respectively. Comparing these natural frequencies with the corresponding values in Tables 2 and 3, one can realize the significant effects of the shear deformation, rotary inertia and the axis extensibility, especially, for the higher modes. For instance, the non-dimensional fundamental natural frequency for the pinned–pinned circular

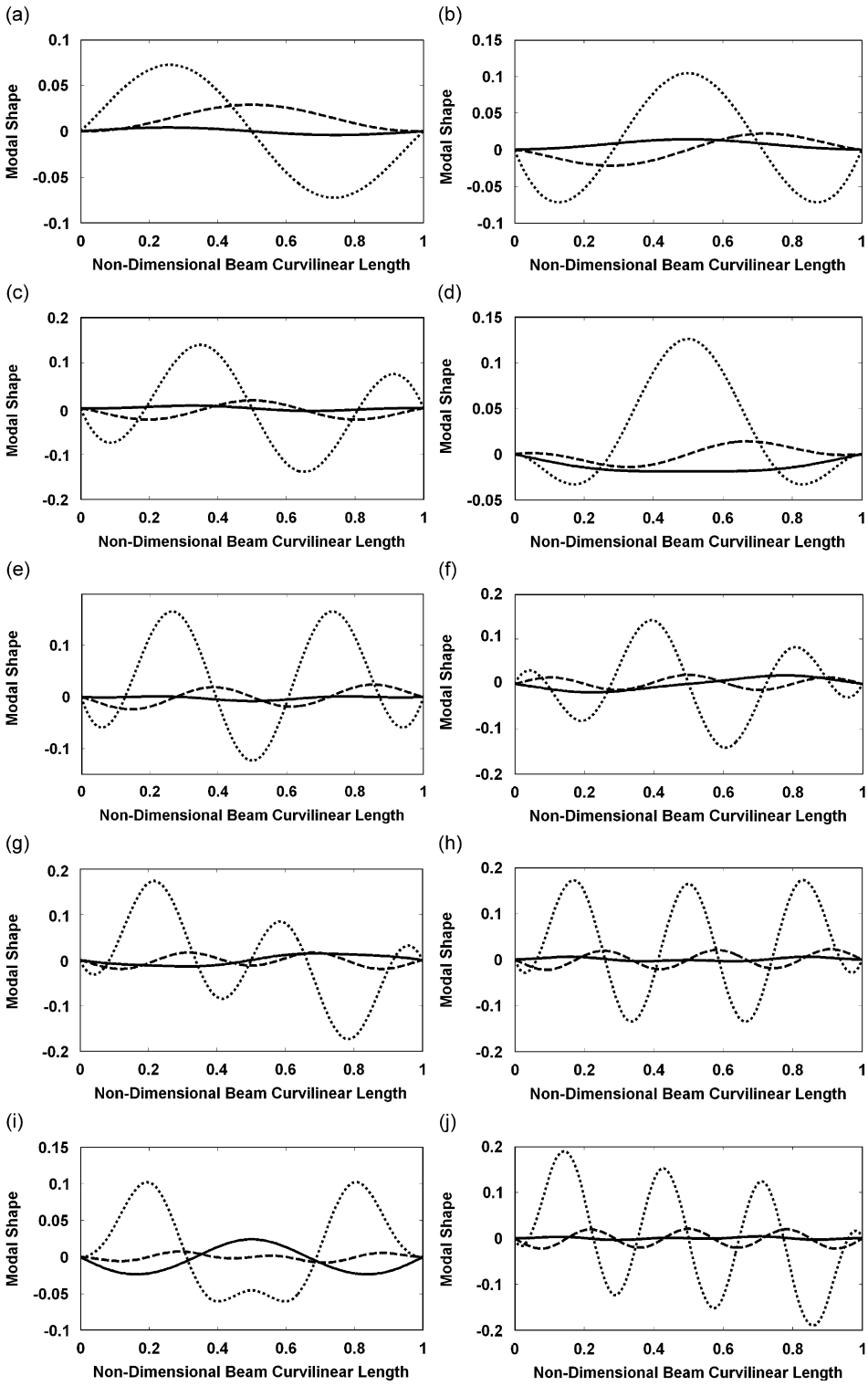

Fig. 4. The first 10 vibration modal shapes of uniform circular curved beam with clamped–clamped boundary conditions. Solid, dashed and dotted lines represent mode shapes for u, w and ψ, respectively: (a) the first mode, (b) the second mode, (c) the third mode, (d) the forth mode, (e) the fifth mode, (f) the sixth mode, (g) the seventh mode, (h) the eighth mode, (i) the ninth mode and (j) the tenth mode.

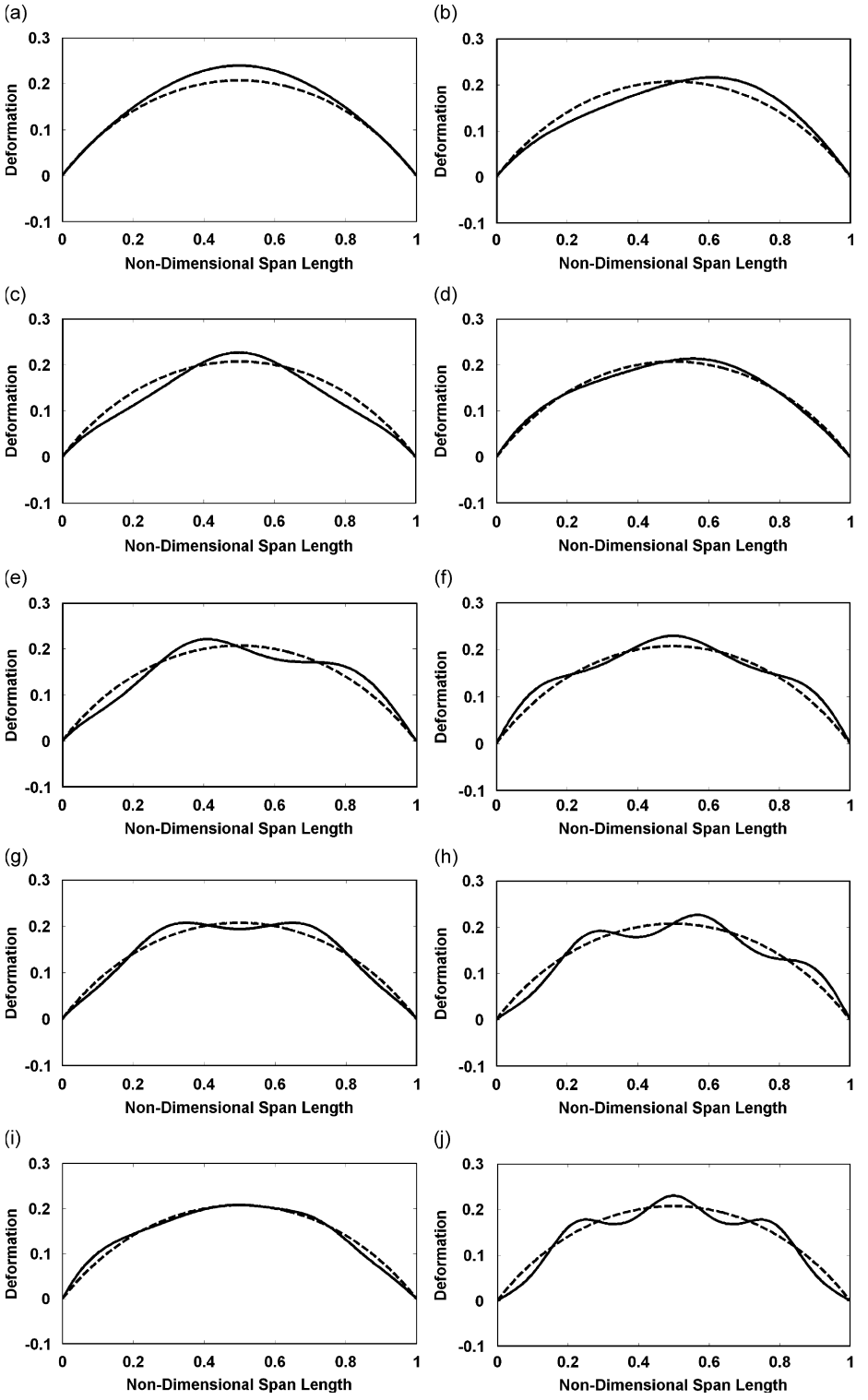

Fig. 5. The deformations relative to the first 10 vibration modes for uniform circular curved beam with clamped–clamped boundary conditions. Solid and dashed lines represent deformed and undeformed configuration: (a) the first mode, (b) the second mode, (c) the third mode, (d) the forth mode, (e) the fifth mode, (f) the sixth mode, (g) the seventh mode, (h) the eighth mode, (i) the ninth mode and (j) the tenth mode.

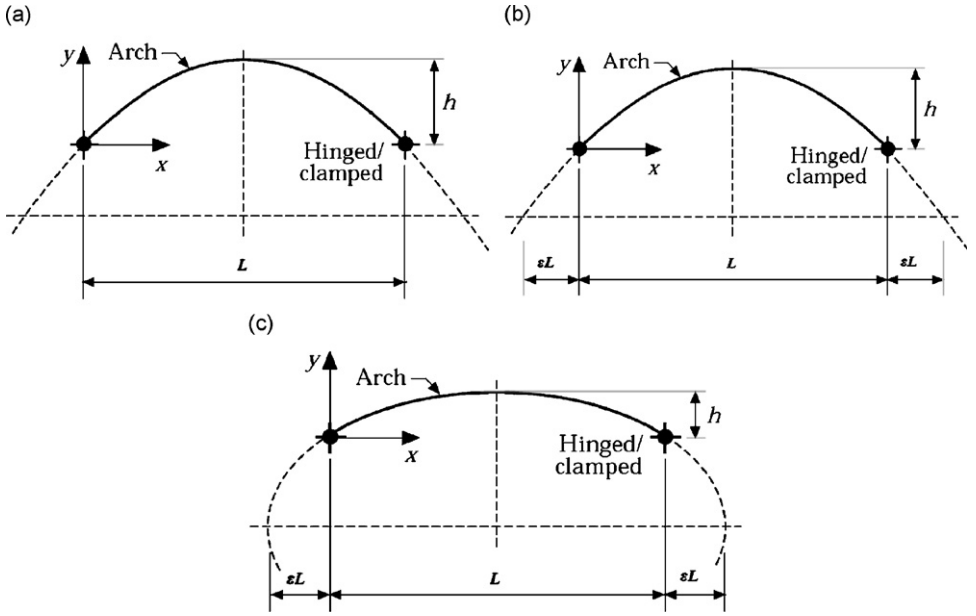

Fig. 6. Different types of curved beams: (a) parabolic, (b) sinusoidal and (c) elliptical.

Table 4
Non-dimensional frequencies, $\lambda = \omega L^2\sqrt{(\gamma A/EI)}$ for the parabolic, elliptical and the sinusoidal curved beams with different boundary conditions (Case 1)

Geometry of arch	Mode	Ref. [17]	Present study
Parabolic	1	21.83	21.759
Hinged–hinged	2	56.00	55.493
$f = 0.3$, SR = 75	3	102.3	100.701
$k_qG/E = 0.3$	4	113.4	113.302
Elliptic ($\varepsilon = 0.5$)	1	35.25	34.892
Hinged–clamped	2	57.11	56.766
$f = 0.2$, SR = 50	3	83.00	81.420
$k_qG/E = 0.3$	4	128.2	124.288
Sinusoid ($\varepsilon = 0.5$)	1	56.3	56.083
Clamped–clamped	2	66.14	66.047
$f = 0.1$, SR = 100	3	114.3	113.406
$k_qG/E = 0.3$	4	181.7	179.264

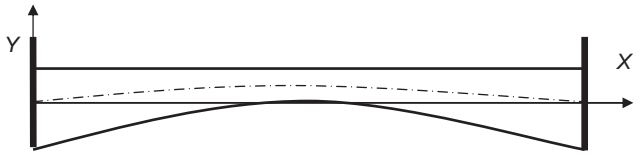

Fig. 7. General non-uniform and non-circular curved beams representing an overpass bridge.

Table 5
Properties of the general non-uniform and non-circular curved beams

Elastic modulus (E)	70 (GPa)	Shear coefficient (k_q)	0.8438
Shear modulus (G)	24.50 (GPa)	Beam width	2 (m)
Density (γ)	2777 (kg/m^3)	Beam span length	40 (m)
Beam upper and lower surface functions	$y = 2(m)$, $y = -0.005x^2 + 0.2x - 2(m)$		
Central line function	$y = -0.0025x^2 + 0.1x(m)$		

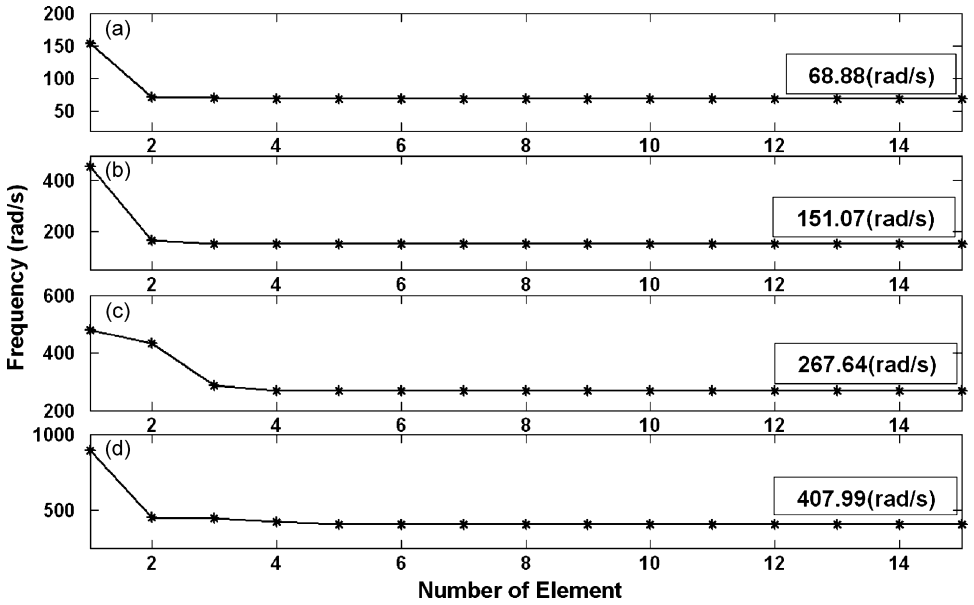

Fig. 8. Convergence analysis for the clamped–clamped general non-uniform and non-circular curved beams: (a) first natural frequency, (b) second natural frequency, (c) third natural frequency and (d) forth natural frequency.

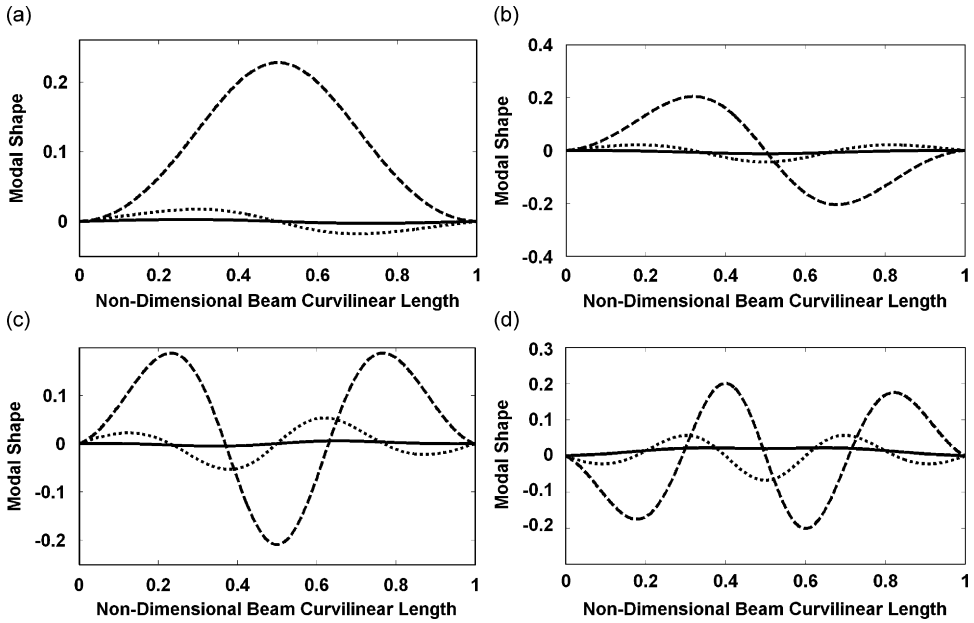

Fig. 9. The first four vibration modal shapes of the general non-uniform and non-circular curved beams with the clamped–clamped boundary conditions. Solid, dashed and dotted lines represent mode shapes for u, w and ψ, respectively: (a) the first mode, (b) the second mode, (c) the third mode and (d) the forth mode.

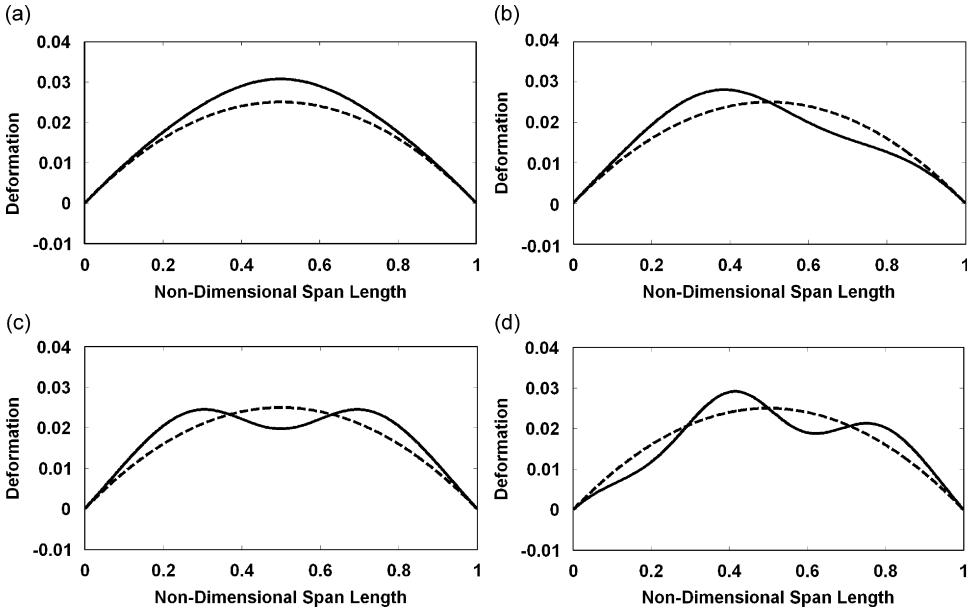

Fig. 10. The deformations of the first four vibration mode for the general non-uniform and non-circular curved beams with the clamped–clamped boundary conditions. Solid and dashed lines represent deformed and undeformed configuration: (a) the first mode, (b) the second mode, (c) the third mode and (d) the forth mode.

Table 6
Non-dimensional natural frequencies $\lambda = \omega R^2\sqrt{(\gamma A/EI)}$ of a uniform circular beam with the pinned–pinned boundary conditions (Case 2)

Mode	$\Phi = 20^\circ$ Ref. [1]	$\Phi = 20^\circ$ Present	$\Phi = 40^\circ$ Ref. [1]	$\Phi = 40^\circ$ Present	$\Phi = 80^\circ$ Ref. [1]	$\Phi = 80^\circ$ Present	$\Phi = 120^\circ$ Ref. [1]	$\Phi = 120^\circ$ Present	$\Phi = 160^\circ$ Ref. [1]	$\Phi = 160^\circ$ Present	$\Phi = 90^\circ$
1	323.000	322.504	80.000	79.876	19.250	19.219	8.000	7.986	4.063	4.0548	37.016
2	690.898	689.840	172.005	171.741	42.283	42.217	18.261	18.232	9.855	9.839	81.951
3	1295.000	1293.040	323.000	322.510	80.000	79.878	35.000	34.946	19.250	19.2194	155.475
4	1988.835	1985.919	496.470	495.741	123.379	123.197	54.288	54.207	30.107	30.061	240.080
5	2915.000	2911.130	728.000	727.033	181.250	181.008	80.000	79.893	44.563	44.502	352.970
6	3933.560	3929.422	982.646	981.612	244.917	244.660	108.301	108.187	60.485	60.421	477.276
7	5183.000	5180.590	1295.000	1294.398	323.000	322.850	143.000	142.9344	80.00	79.963	629.9681
8	6525.941	6528.959	1630.739	1631.495	406.938	407.127	180.309	180.394	100.988	101.037	794.555
9	8099.000	8088.996	2024.000	2021.499	505.250	504.625	224.000	223.722	125.563	125.406	984.949
10	9766.176	9813.830	2440.797	2452.714	609.452	612.435	270.314	271.642	151.615	152.365	1195.491

Table 7
Non-dimensional natural frequencies $\lambda = \omega R^2\sqrt{(\gamma A/EI)}$ of a uniform circular beam with the clamped–clamped boundary conditions (Case 2)

Mode	$\Phi = 20^\circ$ Ref. [1]	$\Phi = 20^\circ$ Present	$\Phi = 40^\circ$ Ref. [1]	$\Phi = 40^\circ$ Present	$\Phi = 80^\circ$ Ref. [1]	$\Phi = 80^\circ$ Present	$\Phi = 120^\circ$ Ref. [1]	$\Phi = 120^\circ$ Present	$\Phi = 160^\circ$ Ref. [1]	$\Phi = 160^\circ$ Present	$\Phi = 90^\circ$
1	505.404	504.629	125.792	125.599	30.894	30.846	13.328	13.307	7.190	7.178	59.861
2	910.100	908.710	226.910	226.563	56.114	56.028	24.488	24.450	13.423	13.402	108.996
3	1639.391	1636.934	409.204	408.590	101.658	101.505	44.707	44.637	24.775	24.737	197.785
4	2374.823	2371.427	593.043	592.194	147.598	147.386	65.109	65.015	36.239	36.186	287.370
5	3421.348	3417.154	854.661	853.612	219.989	212.727	94.161	94.045	52.572	52.507	414.964
6	4483.458	4479.737	1120.178	1119.249	279.358	279.127	123.651	123.549	69.154	69.097	544.627
7	5851.325	5851.922	1462.137	1462.288	364.841	364.880	161.638	161.657	90.517	90.529	712.086
8	7238.872	7256.401	1809.018	1813.407	451.555	452.656	200.173	200.666	112.189	112.469	883.499
9	8929.311	8930.239	2231.623	2231.859	557.201	557.263	247.123	247.153	138.596	138.615	1087.778
10	10,641.76	10,687.974	2659.730	2671.290	664.224	667.119	294.686	295.976	165.348	166.076	1302.309

Table 8
Non-dimensional natural frequencies $\lambda = \omega R^2\sqrt{(\gamma A/EI)}$ of a uniform curved beam with the clamped–pinned boundary conditions (Case 2)

Mode	$\Phi = 20^\circ$ Ref. [1]	$\Phi = 20^\circ$ Present	$\Phi = 40^\circ$ Ref. [1]	$\Phi = 40^\circ$ Present	$\Phi = 80^\circ$ Ref. [1]	$\Phi = 80^\circ$ Present	$\Phi = 120^\circ$ Ref. [1]	$\Phi = 120^\circ$ Present	$\Phi = 160^\circ$ Ref. [1]	$\Phi = 160^\circ$ Present
1	407.417	407.417	101.203	101.203	24.652	24.652	10.482	10.481	5.529	5.528
2	797.909	797.912	198.816	198.817	49.045	49.045	21.312	21.312	11.608	11.608
3	1460.549	1460.585	364.441	364.451	90.415	90.417	39.670	39.671	21.911	21.911
4	2178.817	2178.995	544.006	544.051	135.304	135.315	59.619	59.624	33.130	33.132
5	3161.588	3162.378	789.684	789.882	196.709	196.758	86.899	86.921	48.465	48.478
6	4205.315	4207.747	1050.615	1051.224	261.940	262.093	115.890	115.958	64.772	64.811
7	5510.606	5517.811	1376.930	1378.732	343.511	343.963	152.137	152.339	85.157	85.271
8	6879.112	6897.378	1719.056	1723.625	429.041	430.186	190.150	190.661	106.539	106.827
9	8507.617	8520.880	2126.177	2129.496	530.817	531.649	235.380	235.752	131.977	132.188
10	10,200.606	10,262.610	2549.424	2564.929	636.629	640.509	282.407	284.135	158.430	159.404

Table 9
Non-dimensional natural frequencies $\lambda = \omega R^2\sqrt{(\gamma A/EI)}$ of a uniform circular beam with the clamped–free boundary conditions (Case 2)

Mode	$\Phi = 20^\circ$ Ref. [1]	$\Phi = 20^\circ$ Present	$\Phi = 40^\circ$ Ref. [1]	$\Phi = 40^\circ$ Present	$\Phi = 80^\circ$ Ref. [1]	$\Phi = 80^\circ$ Present	$\Phi = 120^\circ$ Ref. [1]	$\Phi = 120^\circ$ Present	$\Phi = 160^\circ$ Ref. [1]	$\Phi = 160^\circ$ Present
1	29.101	29.101	7.462	7.462	2.064	2.064	1.084	1.084	0.766	0.766
2	180.235	180.235	44.611	44.611	10.721	10.721	4.470	4.470	2.315	2.315
3	505.606	505.607	125..845	125.845	30.910	30.910	13.337	13.337	7.197	7.197
4	991.426	991.436	247.243	247.246	61.200	61.200	26.750	26.750	14.696	14.696
5	1639.392	1639.464	409.204	409.222	101.658	101.663	44.707	44.709	24.775	24.776
6	2449.366	2449.709	611.678	611.764	152.257	152.279	67.180	67.189	37.404	37.409
7	3421.348	3422.617	854.661	854.978	212.989	213.069	94.161	94.197	52.572	52.592
8	4555.335	4559.249	1138.147	1139.127	283.851	284.096	125.648	125.757	70.277	70.339
9	5851.325	5862.148	1462.137	1464.845	364.841	365.519	161.638	161.940	90.517	90.688
10	7309.317	7342.488	1826.630	1834.926	455.958	458.036	202.130	203.056	113.290	113.813

beam with $\Phi = 90^\circ$ is 29.306 for Case 1 compared to 37.016 for Case 2, while the 10th natural frequency of the beam is 234.809 for Case 1 compared to 1195.491 for Case 2. Similarly, the non-dimensional fundamental natural frequency for the clamped–clamped circular beam with $\Phi = 90^\circ$ is 36.657 in Case 1 compared to 59.861 in Case 2 while the 10th natural frequency of the beam is 249.320 in Case 1 compared to 1302.309 in Case 2.

4. Conclusions

In this study, the governing differential equations for the general curved beam vibration including and excluding the effects of the extensibility of the curved axis, the shear deformation and the rotary inertia are derived using the Extended-Hamilton principle and were solved using the FE method.

A 'four-node' Lagrangian-type curved beams element has been developed and combined with the curvilinear integral method to solve both the uniform and non-uniform curved beam with variable curvatures. The results for the conventional geometry (circular, parabolic, sinusoidal and elliptical curves) are in excellent agreement with those reported in published literatures. Furthermore, a new 'two-node' curved beam element has been proposed to study the curved beams' deformation relationship excluding the effects of the extensibility of the curved axis, the shear deformation and the rotary inertia. The curvilinear integral method and the 'four-node' Lagrangian-type shape function are utilized to model the geometrical properties of the curved beams. Results obtained are in excellent agreement with those available in literature for different boundary conditions and curve angles. It has been shown that by using the FE method with the appropriate

shape functions, the vibration response of the curved beams with any arbitrary geometry and different boundary conditions can be accurately obtained.

Acknowledgement

The financial support by the Natural Science and Engineering Research Council (NSERC) of Canada to carry out this research is gratefully acknowledged.

Appendix A

Sub-matrices for Eqs. (6b) and (6c) are

$$\mathbf{M}_{ww} = \mathbf{M}_{uu} = \int_{-1}^{1} \gamma A(\eta)\mathbf{N}(\eta)^{\mathrm{T}}\mathbf{N}(\eta)J_{oc}(\eta)\,\mathrm{d}\eta, \tag{A.1}$$

$$\mathbf{M}_{\psi\psi} = \int_{-1}^{1} \gamma I(\eta)\mathbf{N}(\eta)^{\mathrm{T}}\mathbf{N}(\eta)J_{oc}(\eta)\,\mathrm{d}\eta, \tag{A.2}$$

$$\mathbf{K}_{ww} = \int_{-1}^{1} \left\{ k_q GA(\eta)\mathbf{B}(\eta)^{\mathrm{T}}\mathbf{B}(\eta)J_{oc}^{-1}(\eta) + \frac{EA(\eta)}{\rho(\eta)^2}\mathbf{N}(\eta)^{\mathrm{T}}\mathbf{N}(\eta)J_{oc}(\eta) \right\} \mathrm{d}\eta, \tag{A.3}$$

$$\mathbf{K}_{wu} = \mathbf{K}_{uw}^{\mathrm{T}} = \int_{-1}^{1} \left\{ \frac{EA(\eta)}{\rho(\eta)}\mathbf{N}(\eta)^{\mathrm{T}}\mathbf{B}(\eta) - \frac{k_q GA(\eta)}{\rho(\eta)}\mathbf{B}(\eta)^{\mathrm{T}}\mathbf{N}(\eta) \right\} \mathrm{d}\eta, \tag{A.4}$$

$$\mathbf{K}_{w\psi} = \mathbf{K}_{\psi w}^{\mathrm{T}} = -\int_{-1}^{1} k_q GA(\eta)\mathbf{B}(\eta)^{\mathrm{T}}\mathbf{N}(\eta)\,\mathrm{d}\eta, \tag{A.5}$$

$$\mathbf{K}_{uu} = \int_{-1}^{1} EA(\eta)\mathbf{B}(\eta)^{\mathrm{T}}\mathbf{B}(\eta)J_{oc}^{-1}(\eta) + \frac{k_q GA(\eta)}{\rho(\eta)^2}\mathbf{N}(\eta)^{\mathrm{T}}\mathbf{N}(\eta)J_{oc}(\eta)]\,\mathrm{d}\eta, \tag{A.6}$$

$$\mathbf{K}_{u\psi} = \mathbf{K}_{\psi u}^{\mathrm{T}} = \int_{-1}^{1} \frac{k_q GA(\eta)}{\rho(\eta)}\mathbf{N}(\eta)^{\mathrm{T}}\mathbf{N}(\eta)J_{oc}(\eta)\,\mathrm{d}\eta, \tag{A.7}$$

$$\mathbf{K}_{\psi\psi} = \int_{-1}^{1} EI(\eta)\mathbf{B}(\eta)^{\mathrm{T}}\mathbf{B}(\eta)J_{oc}^{-1}(\eta)\,\mathrm{d}\eta + \int_{-1}^{1} k_q GA(\eta)\mathbf{N}(\eta)^{\mathrm{T}}\mathbf{N}(\eta)J_{oc}(\eta)\,\mathrm{d}\eta. \tag{A.8}$$

References

[1] J. Henrych, *The Dynamics of Arches and Frames*, Elsevier, New York, 1981.
[2] N.M. Auciello, M.A. De. Rosa, Free vibrations of circular arches: a review, *Journal of Sound and Vibration* 176 (4) (1994) 433–458.
[3] W. Austin, A. Veletsos, Free in-plane vibrations of circular arches, *Journal of Engineering Mechanics ASCE* 98 (1972) 311–329.
[4] J.A. Wolf, Natural frequencies of circular arches, *Journal of the Structural Division ASCE* 97 (1971) 2337–2350.
[5] M. Eisenberger, E. Efraim, In-plane vibrations of shear deformable curved beams, *International Journal for Numerical Methods in Engineering* 52 (2001) 1221–1234.
[6] Z. Friedman, J.B. Kosmatka, An accurate two-node finite element for shear deformable curved beams, *International Journal for Numerical Methods in Engineering* 41 (1998) 473–498.
[7] K. Kang, C. Bert, H. Striz, Vibration analysis of shear deformation circular arches by the differential quadrature method, *Journal of Sound and Vibration* 181 (2) (1995) 353–360.
[8] T. Irie, G. Yamada, I. Takahashi, The steady state in-plane response of a curved Timoshenko beam with internal damping, *Ingenieur-Archiv* 49 (1980) 41–49.
[9] V. Yildirim, A computer program for the free vibration analysis of elastic arcs, *Computers and Structures* 62 (3) (1997) 475–485.
[10] A. Veletsos, W. Austin, Free vibration of arches flexible in shear, *Journal of Engineering Mechanics, ASCE* 99 (1973) 735–753.

[11] M.S. Issa, T.M. Wang, B.T. Hisao, extensional vibrations of continuous circular curved beams with rotary inertia and shear deformation: free vibration, *Journal of Sound and Vibration* 114 (2) (1987) 297–308.
[12] P.A.A. Laura, De.I. Verniere, A note in in-plane vibrations of arch-type structures of non-uniform cross-section: the case of linearly varying thickness, *Journal of Sound and Vibration* 124 (1) (1988) 1–12.
[13] X. Tong, N. Mrad, B. Tabarrok, In-plane vibration of circular arches with variable cross-sections, *Journal of Sound and Vibration* 212 (1) (1998) 121–140.
[14] H. ÖztÜrk, İ. Yeşilyurt, M. Sabuncu, In-plane stability analysis of non-uniform cross-section sections, *Journal of Sound and Vibration* 296 (1-2) (2006) 277–291.
[15] S.Y. Lee, J.Y. Hsiao, Free in-plane vibrations of curved non-uniform beams, *Acta Mechanica* 155 (2002) 173–189.
[16] Y.P. Tseng, C.S. Huang, C.J. Lin, Dynamic stiffness analysis for in-plane vibrations of arches with variable curvature, *Journal of Sound and Vibration* 207 (1) (1997) 15–31.
[17] S.J. Oh, B.K. Lee, I.W. Lee, Natural frequencies of non-circular arches with rotatory inertia and shear deformation, *Journal of Sound and Vibration* 219 (1) (1999) 23–33.
[18] P. Raveendranath, G. Singh, B. Pradhan, Free vibration of arches using a curved beam element based on a coupled polynomial displacement field, *Computers and Structures* 78 (2000) 583–590.
[19] P. Litewka, J. Rakowski, Free vibrations of shear-flexible and compressible arches by FEM, *International Journal for Numerical Methods in Engineering* 52 (2001) 273–286.
[20] J.S. Wu, L.K. Chiang, Free vibration analysis of arches using curved beam elements, *International Journal for Numerical Methods in Engineering* 58 (2003) 1907–1936.
[21] M. Petyr, C.C. Fleischer, Free vibration of a curved beam, *Journal of Sound and Vibration* 18 (1971) 17–30.
[22] R. Davis, R.D. Henshell, G.B. Warburton, Constant curvature beam finite elements for in-plane vibration, *Journal of Sound and Vibration* 25 (1972) 561–576.
[23] J. Stoer, R. Bulirsch, *Introduction to Numerical Analysis*, Springer, New York, 2002.